Light-driven growth of nanostructures

E. Jurdik, F. Bentivegna, A.V. Petukhov, A. van Etteger, M. van Rij, W.L. Meerts, Th. Rasing, H. van Kempen

Reasearch Institute for Materials, University of Nijmegen, Toernooiveld 1, 6525 ED Nijmegen, The Netherlands

Laser focusing of neutral atoms in a near-resonant standing wave (an array of "atomic lenses") can be used to produce high resolution, nanometer-scale, regular structures. Atom optical calculations are a powerful tool to understand the processes which govern the light-driven deposition of such nanostructures and thus to improve their resolution and contrast. We present our calculations based on a Monte Carlo scheme and the semiclassical trajectory tracing method. The influence of aberrations of an atomic lens is discussed. Surface diffusion is accounted for by a temperature dependent, stochastic Arrhenius model.

The manipulation of neutral atoms with near-resonant laser light has been shown to be a powerful tool for nanostructure fabrication. Nanolithography using forces exerted by light on atoms in a standing wave radiation field has attracted a lot of attention in several laboratories worldwide. The first direct evidence of the ability of atom optics to serve as a useful means of nanostructuring was demonstrated by Timp *et al.* in 1992 [1]. They focused neutral sodium atoms in the standing wave into a grating-like structure on a substrate. The spacing between the sodium lines was determined by the light diffraction from the structure and was shown to be 294 nm corresponding to the half of the wavelength of the SW used for focusing. In 1993 McClelland *et al.* [2] performed one-dimensional focusing of chromium atoms. Atomic force microscopy showed that the resulting nanostructure consisted of a series of narrow lines with a spacing of 213 nm, a height of 34 nm and a width of 65 nm. McGowan *et al.* [3] created structures of aluminum and Drodofsky *et al.* [4] of chromium. Recent experiments of Natarajan *et al.* [5] have shown that light force cylindrical lenses can be used to focus a thermal sodium beam with an extremely high resolution of 20 nm and a high contrast of about 10:1. Gupta *et al.* [6] and Drodofsky *et al.* [4] extended the geometry of nanolithography experiments and produced two-dimensional nanostructures consisting of equidistantly spaced chromium features.

An important part of applying atom optics to nanostructure fabrication is performing theoretical estimates and computer experiments. These can range from simple analogies with paraxial particle optics [7] to quantum Monte Carlo schemes [8] through time-dependent semiclassical calculations of atomic trajectories [9].

The exact solution of problems involving interaction of atoms with light can be quite complicated and intricate. Nonetheless, the light force on a neutral atom can be split into two terms [10,11]. The conservative (velocity independent) term is called dipole force and can be thought to be a consequence of the interaction of the induced atomic dipole moment with the gradient in the light intensity. The non-conservative (velocity dependent) term is called spontaneous force and is related to the directed absorption of photons from the field and the consequent isotropic spontaneous emission of photons.

Assuming one-dimensional experimental geometry as it is depicted in *Fig. 1*, the semiclassical (net average) force acting on a two-level atom in the standing wave radiation field takes (to the first order in velocity) the form [10]

$$\langle f(x)\rangle = \frac{\hbar p(x)}{1+p(x)}\, k\Delta \tan(kx)\times \qquad (1)$$
$$\left[1+(k\dot{x})\frac{\Gamma^2[1-p(x)]-2p(x)^2(\Delta^2+\Gamma^2/4)}{\Gamma(\Delta^2+\Gamma^2/4)(1+p(x)^2)}\tan(kx)\right],$$

where Δ is the detuning of the laser frequency from the atomic resonance, Γ the natural linewidth of the atomic transition (in radians per second), k the wave number, x the relative transversal position of the atom from the next nearest antinode of the standing wave intensity, and $p(x)$ the saturation parameter related to the light intensity $I(x)$ and the saturation intensity of the atomic transition I_s through

$$p(x) = \frac{\Gamma^2}{\Gamma^2+4\Delta^2}\frac{I(x)}{I_s}. \qquad (2)$$

In the limit of a very large detuning of the standing wave frequency from the atomic resonance the dipole force dominates and the conservative potential is given by

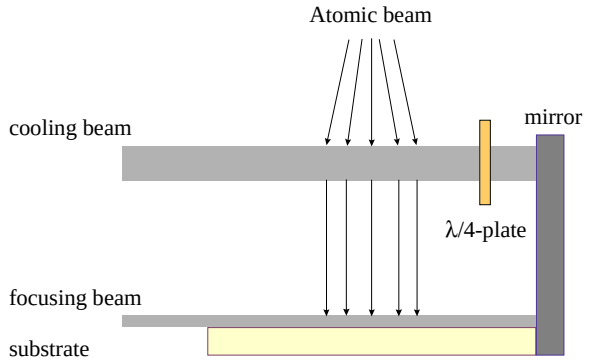

Fig. 1. Schematic of one-dimensional laser focused atomic deposition

$$U(x) = \frac{\hbar\Gamma^2}{8\Delta}\frac{I(x)}{I_s}. \qquad (3)$$

Near its minimum the conservative potential can be approximated by that of a simple harmonic oscillator. In such a harmonic potential the atoms would oscillate with a period T^* independent of their initial transversal position x. By choosing the appropriate interaction time ($t_{\text{int}} = T/4$) with the standing wave light all of them would be focused to the same point on the surface. Such a consideration allows one to define the characteristic points of an atomic lens like they are defined in paraxial optics and to treat all the deviations from these predictions as aberrations [7].

However, the influence of the non-conservative (velocity dependent) part of the light force on the motion of the atoms in the standing wave can be quite substantial providing long interaction times [9]. Besides, a realistic atomic beam always exhibits some spread in longitudinal velocities and thus a spread in interaction times.

We simulated laser focused atomic deposition using a Monte Carlo scheme based on the semi-classical trajectory tracing method [7].

[*] This period is according to Eq. (3) given by

$$T = \sqrt{\frac{4\Delta\lambda^2 m_a}{\hbar\Gamma^2}\frac{I_s}{I_{\max}}},$$

where $I_{\max}$ is the light intensity at the standing wave antinode

We calculated the trajectories of atoms in the standing wave light by numerical integration of the classical equation of motion

$$\langle f \rangle = m_a \ddot{x} \qquad (4)$$

using the fourth-order Runge-Kutta method [12]. In Eq. (4) m_a is the atomic mass and the force is replaced by the semiclassical expression from Eq. (1). *Fig. 2* illustrates these calculations for a monoenergetic, perfectly collimated chromium beam moving through a standing wave at a wavelength of 425.55 nm with a blue detuning of 500 MHz and a Rabi frequency[†] at the field antinode of 1 GHz. As seen from *Fig. 2*, the trajectories do not all terminate in a node of the standing wave. This is referred to as the *spherical* aberration of the atomic lens. In order to minimize it, one wants to have the potential as harmonic as possible. Large positive detunings result in a more harmonic potential but require higher power to focus atoms. Another limitation follows from the consideration of Eq. (3): the higher the detuning the deeper the potential of the standing wave and the better collimation of the atomic beam required.

The resulting atomic density for this ideal case of a monoenergetic (often referred to as monochromatic), perfectly collimated (with an effective transversal temperature of 0 K) chromium beam is calculated by tracing the trajectories of 10000 atoms within the interval of transversal positions [0,λ/2] (*Fig. 3a*). The initial transversal positions of the atoms are randomly generated over this interval, each position being equally probable. The full width half maximum (FWHM) of the chromium feature is only of 1 nm. The conclusion driven from this simulation is that the effect of spherical aberration is small even when compared to the diffraction limitation which is of the order of 6 nm [7].

The effect of the *chromatic* aberration on the shape of the chromium feature is illustrated in *Fig. 3b*. This arises because of the different interaction times of the different atoms of a thermal beam with the standing wave. Longitudinal velocities are randomly generated according to the Maxwell-Boltzmann distribution for an oven temperature of 1700 °C. The FWHM of the chromium peak observed in *Fig. 3b* is 4 nm.

[†] The Rabi frequency measures the coupling between the atom and the field and is given by [11]

$$\Omega^2 = \frac{\Gamma^2}{2}\frac{I}{I_s}.$$

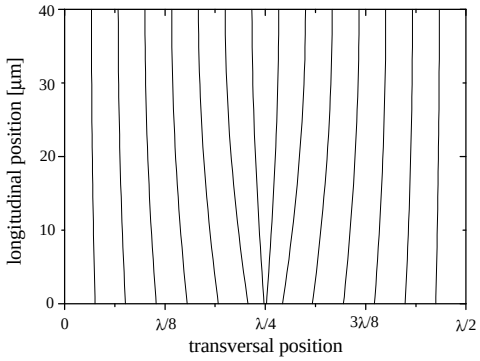

Fig. 2. Calculated trajectories of chromium atoms in the standing wave light for different initial transversal position. The parameters entering these calculations are: a wavelength of the standing wave light of 425.55 nm, a detuning of the standing wave frequency from the atomic resonance of 500 MHz, a Rabi frequency at the field antinode of 1 GHz, a natural linewidth of the atomic transition of 31.4 MHz, an interaction length of chromium atoms with the standing wave of 40 μm, and a longitudinal velocity of chromium atoms of 850 ms^{-1}.

The *divergence* of the atomic beam when entering the standing wave seems to be the most important limitating factor on the focusing properties of an atomic lens. This effect is demonstrated in *Fig. 3c*. The initial transversal velocities are here again randomly generated along the Gaussian distribution [13]. The divergence of the atomic beam was assumed to correspond to an effective transversal temperature of 50 μK. The FWHM of the chromium peak is then increased to about 20 nm.

Low transversal temperatures of an atomic beam can be achieved by means of laser cooling.

Doppler cooling of atoms results from the interaction of the atomic beam with two counter-propagating, red-shifted laser beams. Each beam exerts an average pressure on the atoms in its direction of propagation [14]. An atom moving towards one of these beams is more likely to absorb a photon from the beam because of Doppler effect. A net momentum is transferred to this atom because of the fact that the absorption process is directed while the spontaneous decay is isotropic. Still the achievable low transversal temperature is limited [15] and for the case of chromium atoms is about 120 μK.

A better collimation can be achieved using a transverse polarisation gradient cooling scheme in which the two laser beams have different polarisations to enhance the cooling [14].

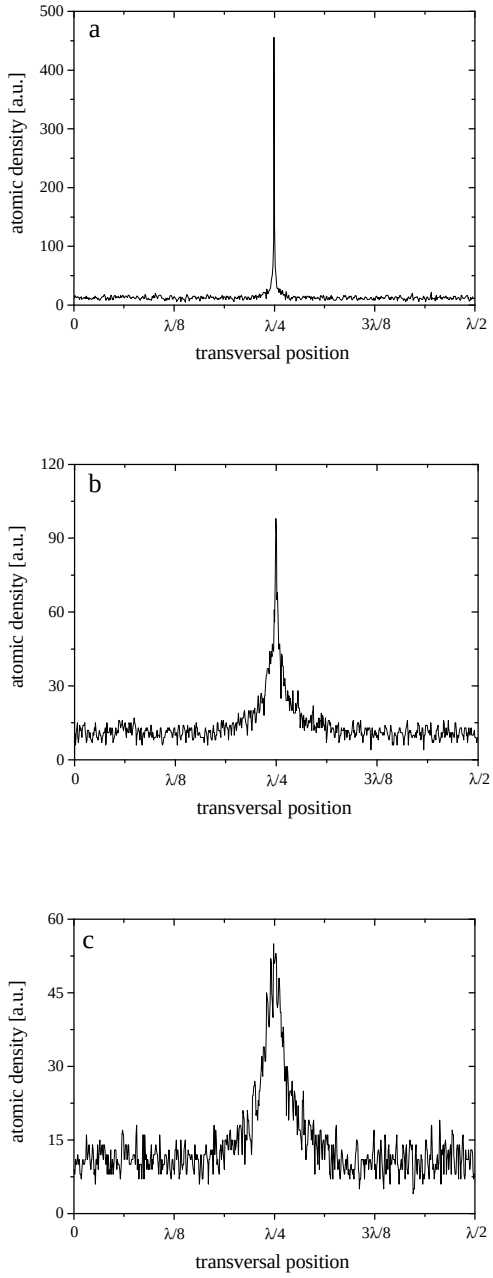

Fig. 3. Resulting atomic densities for a) monoenergetic, perfectly collimated chromium beam, b) a thermal perfectly collimated chromium beam with longitudinal velocities distributed according to the Maxwell-Boltzmann distribution at an oven temperature of 1700 °C, and c) a thermal chromium beam with an effective transversal temperature of 50 μK. The trajectories of 10000 atoms are traced within the depicted interval. All other parameters entering these simulations are the same as those in *Fig. 2*.

In particular, two counterpropagating laser beams, linearly polarised in two perpendicular directions, were used to transversally cool chromium atoms down to an effective transversal temperature of about 25 μK [13,16].

Finally, *surface diffusion* during and after the deposition can be considered to limit the resolution of the structure.

We implemented a stochastic Arrhenius model proposed by Tamborenea and Das Sarma [17] for the simulation of surface diffusion on one-dimensional substrates. In this model three kinetic processes are present: deposition of atoms onto the deposit and two kinds of hopping where one and two bonds are broken via thermal activation (*Fig. 4*). The important parameters in this calculation are the ratios between the one-bond breaking rate and the deposition rate R_{1d}, and between the two-bond breaking rate and the one-bond breaking rate R_{21}. However, the actual values of these parameters are conjectural. Nonetheless, including surface diffusion in our Monte Carlo scheme (i.e. letting the atoms hop during and after the deposition) would give some insight into the effect of surface diffusion on the shape of nanostructures.

The results of our calculation for R_{1d} = 300 and R_{21} = 0.003, and R_{1d} = 12650 and R_{21} = 0.007‡ immediately after the deposition of 10000 atoms are shown in *Fig. 5*. The parameters entering these calculations are the same as those in *Fig. 3*. We conclude that the effect of surface diffusion is mainly to smooth the chromium features. For higher surface temperatures and/or lower activation energies the effect of surface diffusion on the shape and contrast can be very important.

The calculations presented above will serve as a fruitful guide in performing the laser focused deposition of chromium atoms in our laboratory in the near future. Chromium as the first step was chosen because of its excellent stability when exposed to air and its low surface mobility. We are also planning to take into account the quantum character of atom-photon interactions in our simulations.

‡ These values can be thought to correspond to one- and two-bond breaking activation energies of 1.3 eV and 1.6 eV, respectively, a surface temperature of 600 K (solid line in *Fig. 5*) and 700 K (dotted line in *Fig. 5*), respectively, and a deposition rate of 1 monolayer per second.

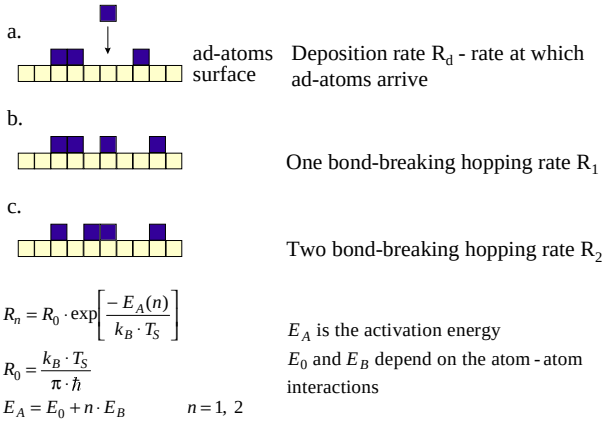

Fig. 4. Schematic representation of the surface diffusion algorithm as implemented in our calculations. Atoms are not allowed to hop up.

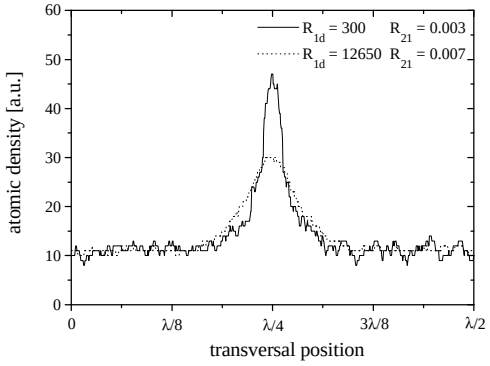

Fig. 5. Effect of surface diffusion on the shape of the structure. All parameters entering these calculations are the same as those in *Fig. 3c*. In addition, atoms are allowed to hop during the deposition process. For further details, see text.

1. G. Timp, R. E. Behringer, D. M. Tennant, J. E. Cunningham, Phys. Rev. Lett. **69**, 1636 (1992).
2. J. J. McClelland, R. E. Scholten, E. C. Palm, R. J. Celotta, Science **262**, 877 (1993).
3. R. W. McGowan, D. Giltner, S. A. Lee, Opt. Lett. **20**, 2535 (1995)
4. U. Drodofsky (private communication).
5. V. Natarajan, , R. E. Behringer, G. Timp, Phys. Rev. A **53**, 4381 (1996).
6. R. Gupta, J. J. McClelland, Z. J. Jabbour, R. J. Celotta, Appl. Phys. Lett. **67**, 1378 (1995).
7. J. J. McClelland, J. Opt. Soc. Am. B **12**, 1761 (1995).
8. P. Marte, R. Dum, R. Taieb, P. D. Lett, P. Zoller, Phys. Rev. Lett. **71**, 1335 (1993).

9. K. K. Berggren, M. Prentiss, G. L. Timp, R. E. Behringer, J. Opt. Soc. Am. B **11**, 1166 (1994).
10. J. P. Gordon and A. Ashkin, Phys. Rev. A **21**, 1606 (1980).
11. J. Dalibard, C. Cohen-Tannoudji, J. Opt. Soc. Am B **2**, 1707 (1985).
12. W. H. Press, S. A. Teukolsky, W. T. Vetterling, B. P. Flannery, Numerical Recipes in C, Cambridge University Press (1992).
13. U. Drodofsky, M. Drewsen, T. Pfau, S. Nowak, J. Mlynek, Microelectronic Engineering **95**, 383 (1996).
14. C. N. Cohen-Tannoudji and W. D. Phillips, Physics Today **10**, 33 (1990).
15. L. Mandel and E. Wolf, Optical Coherence and quantum optics, Cambridge University Press (1995).
16. R. E. Scholten, R. Gupta, J. J. McClelland, R. J. Celotta, Phys. Rev. A **55**, 1331 (1997).
17. P. I. Tamborenea and S. Das Sarma, Phys. Rev. E **48**, 2575 (1993).